Novel fiber Bragg grating fabrication system for long gratings with independent apodization and with local phase and wavelength control

K. M. Chung,[1,*] L. Dong,[2] C. Lu,[3] and H.Y. Tam[1]

[1]*Photonics Research Centre, Department of Electrical Engineering, The Hong Kong Polytechnic University, Hung Hom, Kowloon, Hong Kong SAR, China*
[2]*COMSET/ECE, Clemson University, 207-A Riggs Hall, Clemson, SC 29634 USA*
[3]*Photonics Research Centre, Department of Electronics and Information Engineering, The Hong Kong Polytechnic University, Hung Hom, Kowloon, Hong Kong SAR, China*
[*]*chungkitman@gmail.com*

Abstract: We proposed and demonstrated a novel practical fiber Bragg grating (FBG) fabrication setup constructed with high performance linear stages, piezoelectric translation (PZT) stages, and a highly stable continuous wave laser. The FBG fabrication system enables writing of long FBGs by a continuous translate–and-write process and allows implementation of arbitrary chirp and apodization. A key innovation is that the local Bragg wavelength is controlled by a simple movement of the phase mask by a PZT in the direction perpendicular to its surface. The focus position of the two writing beams is not changed during the Bragg wavelength change, an intrinsic feature of the design, ensuring simplicity, robustness and stability. Apodization can be achieved by vibrating the phase mask in the direction parallel to its surface by a PZT. Phase steps can also be inserted in FBGs at any desired locations by stepping the same PZT. A long uniform FBG and a linearly chirped FBG are written to demonstrate the performance of the setup.

OCIS codes: (120.3180) Interferometry; (230.1480) Bragg reflectors; (060.3735) Fiber Bragg gratings; (220.1230) Apodization; (060.2310) Fiber optics.

References and links

1. K. O. Hill, Y. Fujii, D. C. Johnson, and B. S. Kawasaki, "Photosensitivity in Optical Fiber Waveguides - Application to Reflection Filter Fabrication," Appl. Phys. Lett. **32**(10), 647–649 (1978).
2. L. Poladian, "Simple grating synthesis algorithm," Opt. Lett. **25**(11), 787–789 (2000).
3. J. Skaar, L. G. Wang, and T. Erdogan, "On the synthesis of fiber Bragg gratings by layer peeling," IEEE J. Quantum Electron. **37**(2), 165–173 (2001).
4. H. P. Li and Y. L. Sheng, "Direct design of multichannel fiber Bragg grating with discrete layer-peeling algorithm," IEEE Photon. Technol. Lett. **15**(9), 1252–1254 (2003).
5. L. Dong and S. Fortier, "Formulation of time-domain algorithm for fiber Bragg grating simulation and reconstruction," IEEE J. Quantum Electron. **40**(8), 1087–1098 (2004).
6. D. Z. Anderson, V. Mizrahi, T. Erdogan, and A. E. White, "Production of in-fibre gratings using a diffractive optical element," Electron. Lett. **29**(6), 566–568 (1993).
7. Y. Qiu, Y. L. Sheng, and C. Beaulieu, "Optimal phase mask for fiber Bragg grating fabrication," J. Lightwave Technol. **17**(11), 2366–2370 (1999).
8. P. E. Dyer, R. J. Farley, and R. Giedl, "Analysis of grating formation with excimer laser irradiated phase masks," Opt. Commun. **115**(3-4), 327–334 (1995).
9. Y. Liu, J. J. Pan, C. Gu, F. Zhou, and L. Dong, "Novel fiber Bragg grating fabrication method with high-precision phase control," Opt. Eng. **43**(8), 1916–1922 (2004).
10. M. Gagné, L. Bojor, R. Maciejko, and R. Kashyap, "Novel custom fiber Bragg grating fabrication technique based on push-pull phase shifting interferometry," Opt. Express **16**(26), 21550–21557 (2008).
11. H. P. Li, M. Li, Y. L. Sheng, and J. E. Rothenberg, "Advances in the design and fabrication of high-channel-count fiber Bragg gratings," J. Lightwave Technol. **25**(9), 2739–2750 (2007).
12. M. Nakamura, C. Komatsu, Y. Masuda, K. Fujita, M. Yamauchi, Y. Mizutani, S. Kimura, Y. Suzaki, T. Yokouchi, K. Nakagawa, and S. Ejima, ""Evolution of optical fiber temperature during fiber Bragg grating fabrication using KrF excimer laser," Japn. J. Appl. Phys. **43**, 147–151 (2004).

#146220 - $15.00 USD Received 19 Apr 2011; revised 8 Jun 2011; accepted 9 Jun 2011; published 15 Jun 2011

1. Introduction

Fiber Bragg grating (FBG) is a periodic refractive index perturbation along an optical fiber. It was first demonstration by Hill *et al.* in 1978 [1]. Since then, various FBG fabrication techniques have been developed. Recently, FBGs are becoming a critical element for applications in sensors and optical communication systems. High quality FBGs are immensely useful in a variety of applications. In principle, FBGs with complicated designs are capable of providing optical filters that meet complex spectral and dispersion requirements. However, only few grating structures could be fabricated due to the limitation of effective grating fabrication methods. Design software based on inverse scattering approaches has been well developed [2–5]. With these new complicated design tools for gratings, a practical effective FBG fabrication setup capable of varying both apodization and local grating phase is highly desirable. Most FBGs are fabricated by standard phase mask technique where a photosensitive fiber is placed behind a phase mask [6–8]. The technique is simple and effective. However, it also limits the implementation of complex gratings. A different phase mask has to be made to write each grating with slightly different designs. The cost for a non-standard phase mask is very high.

Several years ago Liu *et al*. demonstrated an excellent approach to write arbitrary FBG with a translate-and-write configuration [9]. The setup makes use of the highly stable velocity characteristics of the air-bearing translation stage with the aid of laser encoder. By synchronizing the shutter and translation stage with a pre-generated grating profile, high performance arbitrary FBGs can be written. The writing beam can be scanned by over hundreds of times with limited of errors.

Gagne *et al*. illustrated a push-pull electro-optic modulation scheme [10]. Two electro-optical phase modulators were placed in the two optical paths. Interference pattern are formed in the core of the moving fiber. The setup requires synchronization of the phase modulator and the motor, which translates the fiber. Phase of the fringe pattern, consequently the corresponding phase in the FBG, at any fiber position can be controlled by the pair of phase modulators and the motor. No moving part in optical setup minimizes moving errors in this arrangement.

Li *et al*. showed a high-channel-count FBG fabrication setup that uses non-standard phase mask technique [11]. A special tailor-made phase mask with complicated profile was used. The advantage is that FBG fabrication is simplified by transferring the main challenges to phase mask fabrication.

These techniques have been applied to many new applications requiring more sophisticated FBG designs, such as multichannel dispersion compensation for telecommunication, multichannel fiber laser and DFB fiber lasers. We reported a novel fiber Bragg grating (FBG) fabrication setup. The FBG fabrication system is capable of writing long FBGs by a translate–and-write process and allows implementation of FBGs with arbitrary chirp and apodization. The local Bragg wavelength is controlled by a simple movement of the phase mask by a PZT in the direction perpendicular to its surface (Y-axis). Both writing beam focuses are not affected in this process and stay at the same locations on the fiber, an intrinsic property of the design, guaranteeing robustness and stability due to the simplicity of the process. The apodization can be achieved by moving the phase mask in the direction parallel to its surface (X-axis) by a PZT. Phase steps can also be implemented by stepping the X-axis controller. Comparing to writing with fiber right behind the phase mask, this new design allows more focused beam on the fiber and, consequently, faster writing. A long uniform FBG and a linearly chirped FBG are written to demonstrate the performance of the setup.

#146220 - $15.00 USD Received 19 Apr 2011; revised 8 Jun 2011; accepted 9 Jun 2011; published 15 Jun 2011

2. Operation principle

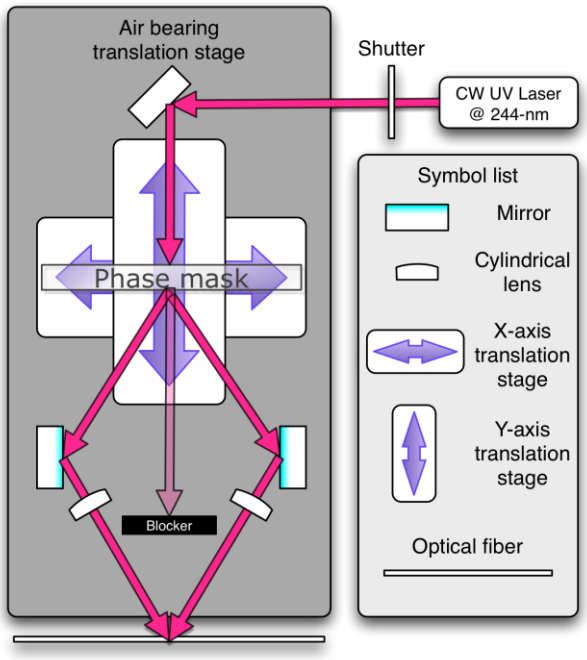

Fig. 1. A schematic diagram of the proposed FBG fabrication setup.

Figure 1 shows a schematic diagram of the proposed FBG fabrication setup. A computer with the software Labview^{TM} controls all the equipment used in this setup, except the laser. This allows synchronization of the control and complicated grating design right in the software for grating realization.

2.1 Equipment

A continuous wave (CW) UV laser (INNOVA Sabre MOTOFRED from coherence Inc.) working at the wavelength of 244-nm with 4-mm coherent length is used as a writing beam. The spot size of the beam is ~1-mm. The laser power is very stable with < ± 1% power variation. The laser power is specified at 500-mW. A phase mask imprinted by holographic pattern technique from Ibsen is used for splitting the writing beam to two beams with half mutual angle of ~13.2° in air with the pitch of 1070.6-nm. The phase mask is mounted on top of two high precision piezoelectric transducers (PZTs) made by Physik Instrumente. The two PZTs are used for controlling the position of the phase mask. The X-axis and Y-axis PZTs have 0.03-nm and 2.5-nm resolution and maximum range of travel of 12-μm and 1500-μm, respectively. The two linear translation stages are controlled by a state-of-the-art controller, which offers integrated, low-noise power amplifier and improves the positioning accuracy to 0.001% of its travel range. The X-axis PZT functions to control the apodization profile or the phase shift of the grating; meanwhile the Y-axis PZT together with a pair of mirrors and cylindrical lenses functions to control the chirp rate or tune the peak wavelength.

The blocker is for blocking the zero-order UV beam from the phase mask. In a typical case, the zero order after passing though the phase mask is ~1%. The two mirrors then reflect the ± 1 order diffraction of the laser beam to the cylindrical lenses. The points of incident of the ± 1 order beams hitting the mirrors change when the phase mask is moved by the Y-axis PZT. Subsequently, the beams incidence on the cylindrical lenses slightly displaced parallel to their optical axes. The fiber is placed at the focus of the two beams. The mutual angle of the two beams at the fiber is changed if the beams hit different parts of the cylindrical lenses, but

#146220 - $15.00 USD Received 19 Apr 2011; revised 8 Jun 2011; accepted 9 Jun 2011; published 15 Jun 2011

the beam position on the fiber is not changed. In the normal case, for writing a non-chirped FBG, the beams pass through the lenses at a fixed mutual angle.

2.1 Operation

In this setup, an FBG is fabricated by a so-called write-and-translate method. In the simplest case, a uniform grating can be written by moving the air-bearing translation stage by the multiples of the grating pitch, Λ. When the shutter is off, the air-bearing translation stage moves the interferometer to next desired position. After sometime for stabilization, the shutter is switched on and the translation stage holds its position and writes the grating. This is the simplest and most direct method to write a grating with CW laser beam. The proportional amount of time used for writing exposure with this approach is extremely high comparing to other translation-and-write methods, and can be controlled by the exposure time on each writing position. The minimum possible off-time is mainly determined by the time taken to stabilize at a given position. In our case, the off time is typically about 700~1300-ms.

The principle of operation is straight forward. However, the implementation of this approach is extremely challenging in practice. It is very hard for the air-bearing translation stage to hold its position within nano-meters scale range for a certain period of time. That is the main reason that other methods used constant velocity while synchronizing the shutter for the purpose of minimizing the phase errors during writing [9,10]. Keeping the position of the stage within as small as ± ~3-nm is impossible without proper environmental isolation and fine-tuning of the air-bearing translation stage. The accuracy of the air-bearing translation stage is heavily relied on the interferometer encoder, which is used for measuring the distance of the translation stage. With 0.3-nm resolution, the stage could in theory have sufficient positional accuracy for negligible phase error in the grating. Any disturbance to the optical path of the interferometer, however, contributes to instability for holding the position. The key of our approach is to achieve high stability. We made improvements on the stability by isolating the environment. Minimal disruption in the setup is thus ensured. Environmental control is the key to keep the air-bearing translation stage working at optimum condition. Proper PID tuning and airflow rate supply to the translation stage also help in stabilizing the stage. After tuning, the stage can stabilize at a position within ± 1-nm for 90% of time within one hour, meanwhile error falls in the range of ± 3-nm for the remaining 10% of the time. The ultra high stability allows a simple, direct and efficient fundamental approach to write high flexible designed FBGs.

In general, for high quality FBGs writing, a CW laser is preferred [9]. There are a number of reasons for adapting a CW laser over a pulse laser. The power stability of pulse lasers is usually worse than that of CW lasers. The fluctuation of output power of a typical pulse laser is usually larger than 3% from pulse to pulse. This causes a large amplitude fluctuation along the grating. Another problem of pulse lasers is the pulse jittering. It results in serious phase errors in the grating. In addition, the peak power of pulse laser is much higher and it significantly reduces the mechanical strength of the fiber [12]. A high mechanical strength is crucial for most FBG sensing applications.

However, using CW laser as writing beam is challenging. Any undesired vibrations in the setup increase the phase error. In normal case, the period of the grating is ~535-nm for a grating in C-band. If there is a relative movement corresponding to π phase shift (267.5-nm) in the grating, the grating can be completely erased. The positional error within ± 3-nm is acceptable. In our setup, over 99% of the time (measured over 20 hours), the error is within ± 3-nm centered at the given position.

The proposed setup not only present an easier and more efficient way to fabricate FBGs, but also offer flexibilities in phase control, which allows arbitrary FBG fabrication, including phase-shift grating and apodized grating, and chirped grating.

The X-axis PZT and a small incremental adjustment of the air-bearing translation stage control the local phase in the grating. In the ideal case, the local phase of the grating during fabrication is only dependent on the position of the phase mask. This assumes that there is no vibration, no temperature difference among the components that affects the optical paths

#146220 - $15.00 USD Received 19 Apr 2011; revised 8 Jun 2011; accepted 9 Jun 2011; published 15 Jun 2011

between the phase mask and the fiber, and no air current moving in the optical paths. The pitch of the phase mask, Λ_{pm} is fixed. The local phase of the grating can be controlled by the position of the phase mask. For example, by moving the X-axis PZT with half of Λ_{pm}, i.e. 535.3-nm in our case, a π phase shift can be produced. A phase shift can also be added by moving the air-bearing translation stage. The advantage of using the PZT instead of the air-bear translation stage is its fast response time. With the ability to change phase along the grating, apodized FBGs can be fabricated. Apodization profile can be achieved by using other less sophisticated FBG fabrication methods, for example, utilization of apodization mask, or scanning with a velocity profile to control the UV dose along the fiber.

2.2 Chirp rate control

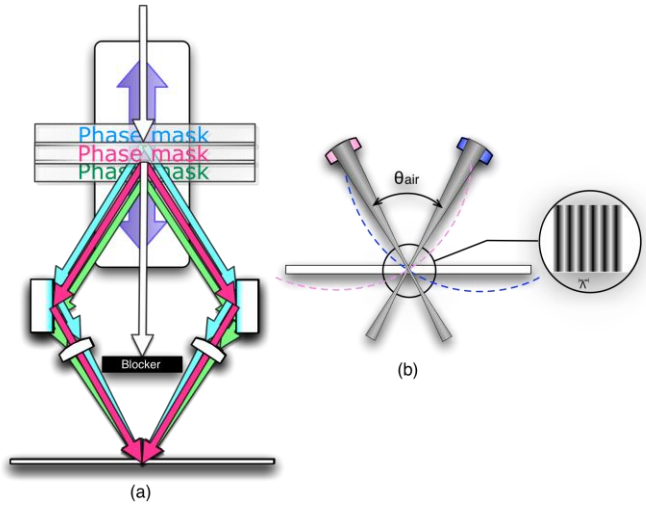

Fig. 2. Illustration of the principle of the grating's pitch changed by the mutual angle of the interference beams. (a) Overall schematic, (b) Detailed illustration about the lenses and beams.

One of the major benefits of this setup is the ability to control the chirp rate of the grating by a simple Y-axis control. The operation principle is illustrated in Fig. 2. The fiber is placed in the focus point of the two beams. The pitch of the grating, Λ, inside the core is determined by the mutual angles of the two beams and described by

$$\Lambda = \frac{\lambda_{uv}}{2\sin\frac{\theta_{air}}{2}}, \tag{1}$$

where λ_{uv} is the wavelength of the UV writing beam, and θ_{air} is the mutual angle of the interference beams. The Bragg wavelength is proportional to the effective refractive index and the pitch, Λ. By tuning the Bragg wavelength slightly during the fabrication, chirp rate can be changed as long as the focal plane of the interference does not change.

Three cases with the phase mask at three different vertical positions are annotated in Fig. 2(a). The optical paths are indicated with red, blue and green color when the phase mask is positioned at the corresponding position, which is labeled with the same color. The red shows the path, which passes though the centre of the cylindrical lens, and the green and blue represent the extreme cases, which obtain the maximum and minimum wavelengths. The relationship of the Bragg wavelength is given by

$$\lambda_B = \frac{n_{eff}\lambda_{uv}}{\sin\frac{\theta_{air}}{2}}. \tag{2}$$

The smaller the mutual angle, the larger the wavelength can be obtained. The cylindrical lenses are placed in such a way that the beams are focused at the core of the fiber. Even if the

#146220 - $15.00 USD Received 19 Apr 2011; revised 8 Jun 2011; accepted 9 Jun 2011; published 15 Jun 2011

beams hit on the sides of the lenses, they are also focused on the same spot as if it hits at centre. It allows the change of the λ_B, or, in the other word, the change of the chirp rate during the writing without the need of re-positioning the fiber vertically. The illustration and calculated results are shown in Fig. 3. In the design, the θ_{air} allows the maximum changes of ~ ± 0.06°, providing ~11.5-nm of wavelength tuning range. Figure 3(c) shows the schematic diagram of the control of the Bragg wavelength. The focal length of the cylindrical lenses was 270-mm. The corresponding calculated maximum deviation of half mutual angle is ~0.1.

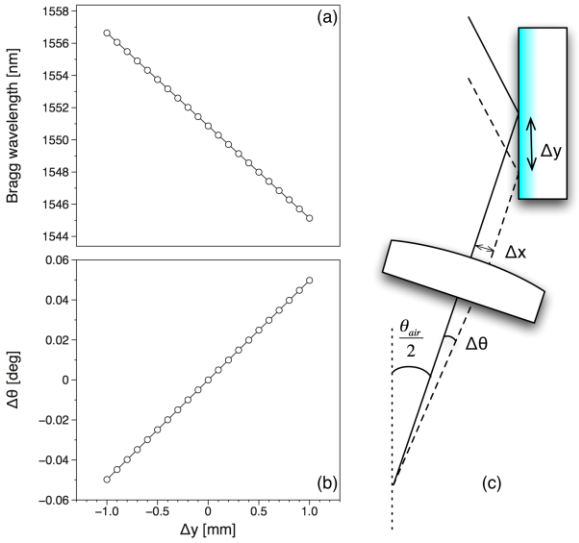

Fig. 3. (a) Bragg wavelength against the change of vertical position of the phase mask, Δy. (b) $\Delta\theta$ against Δy (c) illustration of controlling Bragg wavelength.

The operation principle for making phase shift and chirped FBG has been introduced. The two parameters can be independently and controllably tuned. However, the overall performance relies heavily on the accuracy of the alignments of the components. The mirrors play very important role. The mirrors have to be solidly mounted.

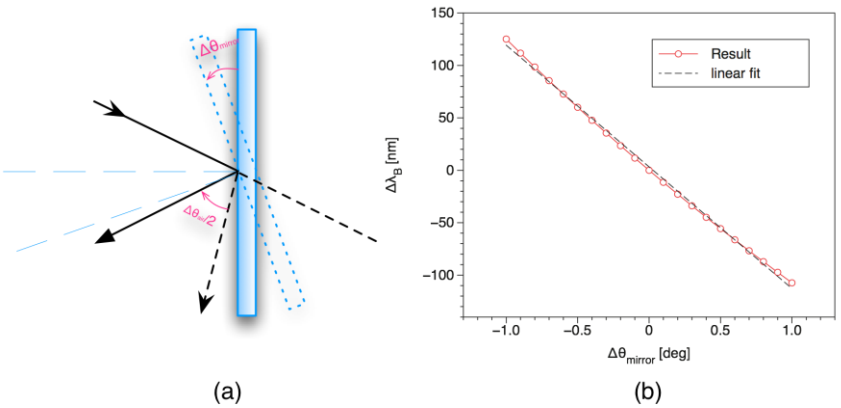

Fig. 4. (a) Illustration of the deviation of angles of the mirrors and the change of the half mutual angle of the interference. (b) Deviation of Bragg wavelength against the deviation of the angle of the mirror

The Bragg wavelength of the grating is very sensitive to the angles of deviations of the mirrors. Figure 4 illustrates the situation when the mirrors accidently moved slightly. The sensitivity is about 116-nm per degree, assuming the angles changes symmetrically. Since the sensitivity is so high that the mirrors have to be solidly mounted and no adjustable mount is

#146220 - $15.00 USD Received 19 Apr 2011; revised 8 Jun 2011; accepted 9 Jun 2011; published 15 Jun 2011

used. A highly stable environment is required. The high stability of the writing environment is reflected on the position of the air-bearing translation stage. Figure 5 shows the position error.

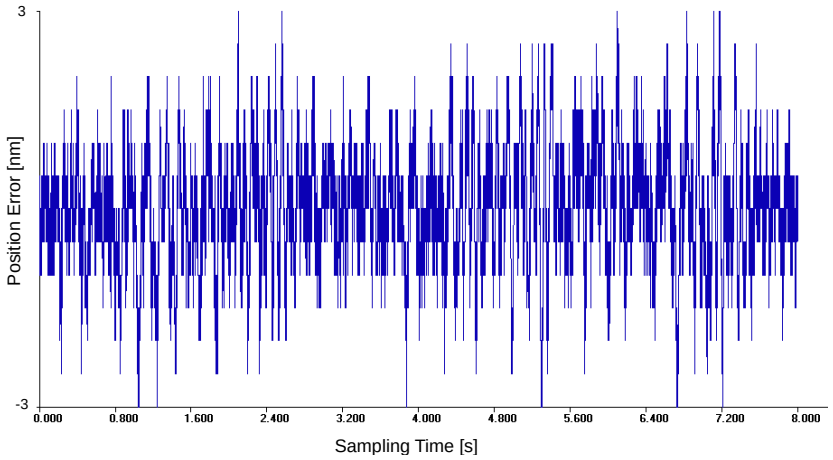

Fig. 5. The position error of the air bearing translation stage.

The error was measured by the software package, Nscope, which is used for tuning the control parameters of the translation stage from Aerotech. The units of Y-axis and X-axis are nanometers and seconds, respectively. The position error was sampled at 1 kHz for 8 seconds. In order to examine its stability, the position error was measured with a laser interferometer encoder from Renishaw's Model RL10. Stability over long duration was also measured. 80.56%, 99.31%, and 99.56% of the error fell in the range of ≤ ± 1-nm, ≤ ± 3-nm and < ± 5-nm, respectively. The raw data was sampled at 1 kHz and measured over 20 hours. Greater than 99% of the time, the air-bearing stage stays at its position with its stability up to ± 3-nm which allows sufficient stability for writing long and highly complex FBGs.

3. Result

3.1 Long FBG

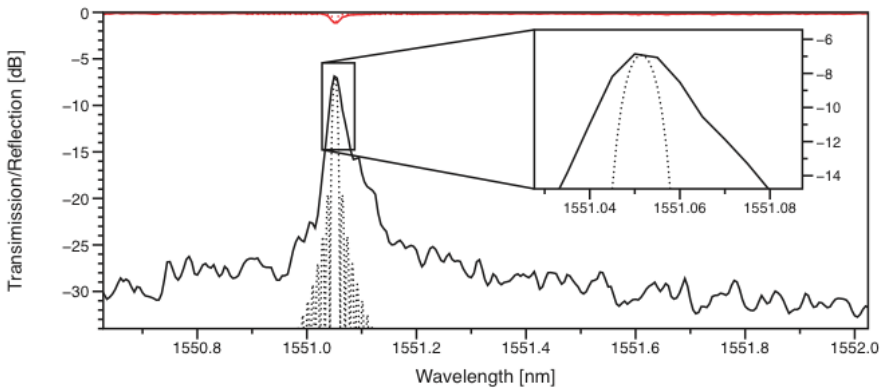

Fig. 6. spectra of a 90-mm long uniform FBG.

The transmission and reflection spectrum of a 90-mm long uniform FBG are shown in Fig. 6. The peak wavelength is 1551.05-nm with ≤15-pm of −3-dB bandwidth. The spectrum of the grating was measured by an MOI interrogator (model SM-125) with the resolution of 5-pm. The laser power was 60-mW with ~1-mm spot size of the beam. The designed grating period, Λ, was 535.155-nm. The dash lines show the simulated spectra. The FBG was fabricated by simple translate-and-write method. When the air-bearing stage was holding at the initial

#146220 - $15.00 USD Received 19 Apr 2011; revised 8 Jun 2011; accepted 9 Jun 2011; published 15 Jun 2011

position, the shutter opened and the laser beams hit at the core of the fiber for three seconds of exposure time. The translation stage then move to 100 times of its pitch, i.e. ~53.5-μm, and then hold its position for a few hundreds of milliseconds in order to ensure the vibration being minimized during seeking for new location, and the beam was on again at this new position. The grating was scanned by one time for a travel length of 90-mm.

The fabrication of long length FBG has been a challenging problem for most FBG fabrication technique. Standard phase mask technique is the most commonly used for writing gratings. The length of the mask limits the grating length. There are two sophisticated techniques for making phase masks. With the phase mask made by electron beam technique, there are phase errors where e-beam fields are stitched together. The resultant grating suffers large phase errors. Phase masks made by holographic exposure are much better in minimizing phase errors. However, the cost for such a long phase mask is very high especially when they have to be made for each grating wavelength.

There are three difficulties for fabricating long FBGs. Two main problems are nanoscopic scale vibrations and temperature fluctuations during the long period of fabrication time. These two issues can be minimized by the isolation of the environment for the whole writing facilities. Additionally, optical alignments and mechanical designs are also critical. The whole setup including the air-bearing translation stage and the fiber holder platform is mounted on a 1.5-ton granite. Under the granite, there are four rubbers to absorb vibration from the ground. The granite is placed on top of Tuned-Damped Field smart table made from Newport. The table measures the high frequency vibration and actively cancels the noise with a built-in damper. Phase error depends strongly on vibrations at any part of the system in an interferometer setup like ours. The alignment of the optical path also plays a critical role.

3.2 Chirped FBG

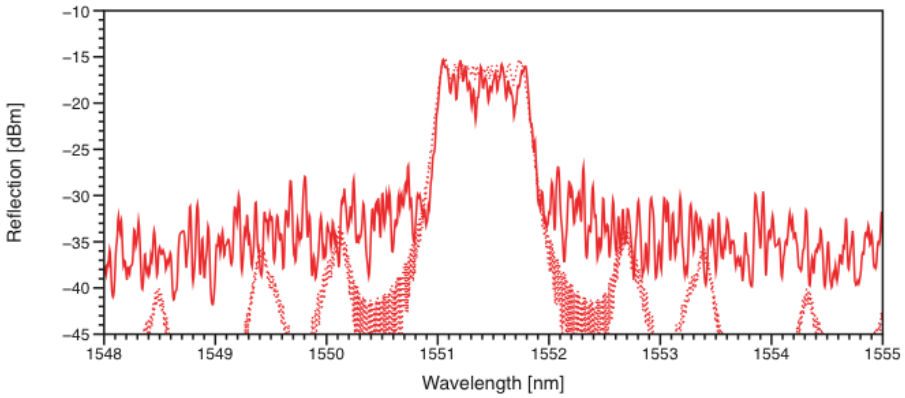

Fig. 7. Reflection spectrum of a 50-mm long chirped grating.

A result of a 50-mm long linear chirped grating is shown in Fig. 7. The dash line shows the simulated result. The chirped rate was 0.15-nm/mm. The exposure time was 3 seconds for one step. One translation step was 20 times of its pitch. This step changes along the fiber as local Bragg wavelength is adjusted by the Y-axis stage.

4.Conclusion

A novel FBG fabrication setup is reported. The system combines stage-of-the-art equipment including laser, PZTs and air-bearing translation stages, with simplicity of independent controls of local Bragg wavelength, phase and apodization for fabricating any arbitrary FBGs. The working principle is reported. Some essential challenges are discussed. This paper reports some preliminary results. The fabrication of a 90-mm long FBG with –3dB bandwidth of less than 15-pm and a 50-mm long chirped FBG with 0.15-nm/mm chirped rates were demonstrated. With the new ability to control phase, apodization and local Bragg wavelength,

#146220 - $15.00 USD Received 19 Apr 2011; revised 8 Jun 2011; accepted 9 Jun 2011; published 15 Jun 2011

a variety of sophisticated FBGs can be fabricated, potentially opening up many new applications which can benefit from FBGs with designs which is difficult to write currently.

Acknowledgments

The authors acknowledge the funding support from the University Grants Council's Matching Grant of the Hong Kong Special Administrative Region Government under the Niche Areas project J-BB9 J.

#146220 - $15.00 USD Received 19 Apr 2011; revised 8 Jun 2011; accepted 9 Jun 2011; published 15 Jun 2011